

# What Bohmian mechanics says about arrival times of 1D vacuum squeezed states

Angel Garcia-Chung\* and Humberto G. Laguna†

Departamento de Química, Universidad Autónoma Metropolitana, San Rafael Atlixco  
No. 186, Iztapalapa, Ciudad de México 09340, México

February 11, 2025

## Abstract

We calculate the time of arrival probability distribution of a quantum particle using the Bohmian formalism. The pilot-wave is given by the wave function of the one dimensional vacuum squeezed state but written in the Schrödinger representation. We made use of the unitary representation of the symplectic group in the Hilbert space  $L^2(\mathbb{R})$ . The solution to the Bohmian equations are analytical function thus allowing for a closed expression of the time of arrival distribution which differs from the counterparts in the standard quantum mechanics formulation.

## 1 Introduction

In classical mechanics, the Time of Arrival (TOA) refers to the time it takes for a particle to travel between two positions along a well-defined trajectory. For a single particle moving in one dimension<sup>1</sup>, the TOA is determined by inverting the Equation of Motion (EoM) to solve for the time parameter. This inversion yields a classical TOA expression dependent on the particle's initial position and momentum. However, this process requires careful consideration of the EoM's monotonicity and range. If the EoM has a bounded range, the resulting TOA expression may only be valid for specific initial conditions; otherwise, mathematical inconsistencies arise.

To illustrate, consider the classical harmonic oscillator described by the EoM given by

$$x(t) = A(x_0, p_0) \cos(\omega t - \phi(x_0, p_0)), \quad (1)$$

where the amplitude  $A(x_0, p_0)$  and phase  $\phi(x_0, p_0)$  depend on the initial conditions  $x_0$  and  $p_0$  as

$$A(x_0, p_0) = \sqrt{x_0^2 + \frac{p_0^2}{m^2\omega^2}}, \quad \phi(x_0, p_0) = \arctan\left(\frac{p_0}{m\omega x_0}\right). \quad (2)$$

The range of the EoM given in Eqn (1) is the interval  $I_{HO} = [-A(x_0, p_0), +A(x_0, p_0)]$  hence, if we seek for the TOA at the position  $x(T) = L$  by inverting Eqn (1), then we must have that  $L \in I_{HO}$  or otherwise the particle will never reach  $L$ . Now notice that for a fixed value  $L$ ,

---

\*alechung@tec.mx

†hlag@xanum.uam.mx

<sup>1</sup>Throughout this work, we consider only one-dimensional single-particle systems.

not all the initial conditions  $(x_0, p_0)$  provide an interval  $I_{HO}$  such that  $L \in I_{HO}$ . Therefore, fixing  $L$  divides the set of initial conditions  $(x_0, p_0)$  into two subsets: one where  $L \in I_{HO}$  thus allowing for finite TOA and another one where  $L \notin I_{HO}$  and the TOA is undefined. This conclusion extends to any bounded one-dimensional trajectory governed by an invertible EoM.

This insight has significant implications for Bohmian mechanics [1, 2, 3] where the TOA probability distribution can be constructed by integrating over initial conditions. Consequently, the splitting of initial conditions into those allowing a finite TOA and those where TOA is undefined inherently shapes the resulting TOA distribution. This work explores how this splitting influences TOA distributions in Bohmian mechanics for the 1D vacuum squeezed state.

In Standard Quantum Mechanics (SQM), particle trajectories are not directly available for TOA calculations. Since the splitting of initial conditions arises from the mathematical properties of EoMs, we can anticipate differences between the TOA predictions in SQM and Bohmian mechanics when analyzing 1D systems with finite-range EoMs. However, it is mathematically possible that a similar splitting could also arise as a consequence of specific operations on the wave function. If this is the case, further analysis is required to identify which wave-function-based TOA formulations in SQM incorporate such a splitting.

Numerous approaches [4, 5, 6, 7, 8, 9, 10, 11] have been proposed to define the TOA in SQM and yet, a definite expression fully satisfactory is still absent. The most recent proposal [12] derives the TOA distribution from the wave function by taking the absolute value of the time derivative of the probability density  $\rho_t(L)$  at a fixed position  $L$ . However, this approach does not account for the range constraints of the EoMs, as discussed earlier. Consequently, for systems with finite-range EoMs (as in our results, Eq. 26), the TOA calculation yields a distinct expression.

Among the most notable proposals to address the TOA in the SQM formalism [5, 7], as well as [13], all encounter mathematical, conceptual or operational problems, such as limitations to specific potentials, reliance on ad hoc regulators, or the use of modified Hamiltonians. However, we hope that as part of future projects, we can delve into the TOA predictions based on these proposals when applied to the one-dimensional vacuum squeezed state.

In the case of the Bohmian formalism, many works have deal with the TOA [14, 15, 16, 17, 18] but so far, none of them consider the 1D vacuum squeezed state [19, 20, 21] as the pilot wave for the Bohm trajectories. The reason may be that squeezed states are mostly analyzed within the Fock representation rather than the Schrödinger representation. The Fock representation is better suited for quantum optics calculations whereas the Schrödinger representation is the appropriate one if we want to consider the Bohmian formalism.

Given these considerations, this work calculates the TOA distribution of the 1D vacuum squeezed state using Bohmian mechanics and examines its expected value. We focus on a system with no detector and analyze the key features of the TOA distribution and its mean value. A central result is that Bohmian trajectories share similarities with classical harmonic oscillator trajectories in that both are bounded. To proceed, we employ the unitary representation of the symplectic group [22, 23, 24, 25] to obtain a position Schrödinger representation of the squeezed state. A direct benefit of this approach is the Gaussian form of the quantum state, which depends on the squeezing parameter and phase. Furthermore, since the quantized system corresponds to a quantum harmonic oscillator, we exploit the fact that its time evolution (at both classical and quantum levels) can be described as a curve in the symplectic group, rendering the results in a closed analytical form. These aspects are discussed in Section 2. Section 3 presents the Bohmian analysis of the time-evolved squeezed state, with particular emphasis on the dependence of Bohmian trajectories on the squeezing parameter and phase. The TOA analysis for Bohmian trajectories follows in Section 4, with a discussion of the results

provided in Section 5.

## 2 Schrödinger representation for squeezed states

In this section we are going to introduce the main mathematical ingredients to obtain a closed expression for the vacuum 1D squeezed state in the Schrödinger representation. We will use this representation for its ease in yielding the explicit form of the Bohm's equations in the next section. To begin with, let us consider the single mode vacuum squeezed operator given by

$$\widehat{S}(\xi) = e^{\frac{1}{2}[\xi^*(\widehat{a})^2 - \xi(\widehat{a}^\dagger)^2]}, \quad (3)$$

where the parameter  $\xi \in \mathbb{C}$  is the squeezing parameter and let us denote its polar and Cartesian forms as  $\xi = r e^{i\phi} = \xi_x + i\xi_y$ . The operator in the exponential of Eqn (3) is the infinitesimal squeezing operator  $\widehat{s}(\xi)$ . It can be written in terms of the position and momentum operators  $\widehat{x}$  and  $\widehat{p}$  as

$$\widehat{s}(\xi) = -\frac{i}{2} \left[ \xi_y \frac{\widehat{x}^2}{l^2} - \xi_x \frac{(\widehat{x}\widehat{p} + \widehat{p}\widehat{x})}{\hbar} - \frac{\xi_y l^2 \widehat{p}^2}{\hbar^2} \right], \quad (4)$$

where we have introduced the proper length  $l = \sqrt{\frac{\hbar}{m\omega}}$ . This was done in order to have the units for the coefficients  $\xi_x$  and  $\xi_y$  compatible with the units for the symplectic group elements as we will see further below. The operator  $\widehat{s}(\xi)$  can be written as

$$\widehat{s}(\xi) = -\frac{i}{2\hbar} \widehat{\vec{R}}^T \mathbf{L}(\xi) \widehat{\vec{R}}, \quad (5)$$

where the array  $\widehat{\vec{R}}$  is given by

$$\widehat{\vec{R}} = \begin{pmatrix} \widehat{x} \\ \widehat{p} \end{pmatrix}, \quad (6)$$

and the symbol  $^T$  is the array transpose and the matrix  $\mathbf{L}(\xi)$  is given as

$$\mathbf{L}(\xi) = \begin{pmatrix} \frac{\hbar \xi_y}{l^2} & -\xi_x \\ -\xi_x & -\frac{l^2 \xi_y}{\hbar} \end{pmatrix}. \quad (7)$$

There exists a Lie algebra isomorphism between operators of the form  $\widehat{s}(\vec{r})$  for general real  $2 \times 2$  symmetric matrices  $\mathbf{L}(\vec{r})$  and the Lie algebra  $sp(2, \mathbb{R})$  of the symplectic group with  $n = 1$  [25]. The isomorphism is given as

$$\iota : sp(2, \mathbb{R}) \rightarrow \mathcal{P}(2, \mathbb{R}); \mathbf{J}\mathbf{L}(\vec{r}) \mapsto \widehat{s}(\vec{r}) \quad (8)$$

where the matrix  $\mathbf{J}$  is of the form

$$\mathbf{J} = \begin{pmatrix} 0 & 1 \\ -1 & 0 \end{pmatrix}. \quad (9)$$

As a result, we can consider the squeezing operator in Eqn (3) to be the unitary representation of a symplectic matrix  $\mathbf{M}(\xi) \in Sp(2, \mathbb{R})$  given as

$$\mathbf{M} = e^{\mathbf{J}\mathbf{L}} = \cosh\left(\sqrt{-\det \mathbf{L}}\right) \mathbf{1}_2 + \frac{\sinh\left(\sqrt{-\det \mathbf{L}}\right) \mathbf{J}\mathbf{L}}{\sqrt{-\det \mathbf{L}}}, \quad (10)$$

where  $\mathbf{1}_2$  stands for the  $2 \times 2$  identity matrix. Notice that in the case of  $\widehat{s}(\xi)$ , we have that  $\det \mathbf{L}(\xi) = -r^2$  hence, the components of the symplectic matrix  $\mathbf{M}(\xi)$  are given as

$$A = [\mathbf{M}(\xi)]_{11} = \cosh(r) - \sinh(r) \cos(\phi), \quad (11)$$

$$B = [\mathbf{M}(\xi)]_{12} = -\frac{l^2 \sinh(r) \sin(\phi)}{\hbar}, \quad (12)$$

$$C = [\mathbf{M}(\xi)]_{21} = -\frac{\hbar \sinh(r) \sin(\phi)}{l^2}, \quad (13)$$

$$D = [\mathbf{M}(\xi)]_{22} = \cosh(r) + \sinh(r) \cos(\phi), \quad (14)$$

and we can check the correct units of the components recalling that the matrix  $\mathbf{M}$  acts linearly upon the phase space vectors, i.e.,  $\mathbf{M}\vec{R} = \vec{R}'$ .

We now use the unitary representation of this symplectic group element and obtain

$$\Psi_\xi(x) = \int \frac{e^{\frac{i}{2\hbar} \left[ \frac{D}{B} x^2 - \frac{2x'x}{B} + \frac{A}{B} x'^2 \right]}}{\sqrt{2\pi i \hbar B}} \Psi_0(x') dx', \quad (15)$$

where the vacuum state  $\Psi_0(x)$  is given by

$$\Psi_0(x) = \left( \frac{1}{\pi l^2} \right)^{1/4} e^{-\frac{x^2}{2l^2}}. \quad (16)$$

The integral in Eqn (15) can be explicitly solved and it provides the analytic expression for the squeezed state written in the Schrödinger representation

$$\Psi_\xi(x) = N e^{-\frac{1}{2} S x^2}, \quad (17)$$

where the coefficients  $N$  and  $S$  are given by

$$N = \left( \frac{1}{\pi l^2} \right)^{1/4} \left( \frac{l^2}{l^2 A + i \hbar B} \right)^{\frac{1}{2}}, \quad (18)$$

$$S = \frac{l^2}{\hbar^2 B^2 + A^2 l^4} - \frac{i}{\hbar} \frac{(l^4 A C + \hbar^2 B D)}{(A^2 l^4 + \hbar^2 B^2)}, \quad (19)$$

respectively. Here we made use of the symplectic group condition

$$\mathbf{J} = \mathbf{M} \mathbf{J} \mathbf{M}^T \quad (20)$$

which in this case implies that  $\det \mathbf{M} = 1$ . Note also that both,  $\Psi_0$  and  $\Psi_\xi$  are normalized.

We now move to the time evolution of the squeezed state given in Eqn (17). The Hamiltonian for the time evolution is given by the quantum harmonic oscillator

$$\widehat{H} = \frac{1}{2m} \widehat{p}^2 + \frac{m\omega^2}{2} \widehat{q}^2, \quad (21)$$

which is used to derive the time evolution operator  $\widehat{U}(t) = e^{-\frac{i}{\hbar} t \widehat{H}}$ . However, the Hamiltonian in Eqn (21) (for a fixed value of  $t$ ) is also an element of the Lie algebra  $sp(2, \mathbb{R})$  where  $\mathbf{L}(H)$  now is given by

$$\mathbf{L}(H) = \begin{pmatrix} m\omega^2 t & 0 \\ 0 & \frac{t}{m} \end{pmatrix}, \quad (22)$$

which, using the relation in Eqn (10) gives a curve  $t \mapsto Sp(2, \mathbb{R})$  in the symplectic group, i.e.,

$$\mathbf{M}_H = \begin{pmatrix} \cos(\omega t) & \frac{l^2}{\hbar} \sin(\omega t) \\ -\frac{\hbar}{l^2} \sin(\omega t) & \cos(\omega t) \end{pmatrix}. \quad (23)$$

As a result, the time evolution of the squeezed state  $\Psi_\xi(x)$  will obey the following relation

$$\Psi_\xi(x, t) = \widehat{U}(t)\Psi_\xi(x, t=0) = \widehat{S}(H, \xi)\Psi_0(x, t=0) \quad (24)$$

where the operator  $\widehat{S}(H, \xi)$  is the unitary operator corresponding to the representation of the symplectic matrix

$$\mathbf{M}(t, \xi) = \mathbf{M}_H \cdot \mathbf{M}(\xi) = \begin{pmatrix} \widetilde{A} & \widetilde{B} \\ \widetilde{C} & \widetilde{D} \end{pmatrix} \quad (25)$$

This route of analysis paves the way to obtain the explicit analytic expression for the time evolved squeezed state which takes a form similar to Eqn (17) but with the matrix coefficients now replaced by those of the matrix  $\mathbf{M}(t, \xi)$  instead. That is to say,  $\Psi_\xi(x, t)$  is given as

$$\Psi_\xi(x, t) = \widetilde{N} e^{-\frac{1}{2}\widetilde{S}x^2} \quad (26)$$

where the coefficients are now given by

$$\widetilde{N} = \left(\frac{1}{\pi l^2}\right)^{1/4} \left(\frac{l^2}{l^2 \widetilde{A} + i\hbar \widetilde{B}}\right)^{1/2} \quad (27)$$

$$\widetilde{S} = \frac{l^2}{\hbar^2 \widetilde{B}^2 + \widetilde{A}^2 l^4} - \frac{i}{\hbar} \frac{(l^4 \widetilde{A} \widetilde{C} + \hbar^2 \widetilde{B} \widetilde{D})}{(\widetilde{A}^2 l^4 + \hbar^2 \widetilde{B}^2)}. \quad (28)$$

The expression for  $\Psi_\xi(x, t)$  is a closed analytic expression which can be used to obtain the exact solution of the Bohm equation for a particle in a Bohm potential guided by the squeezed state  $\Psi_\xi(x, t)$ . In Figure (1) we show a colorbar plot of the square of the wave function  $|\Psi_\xi(x, t)|^2$ . It can be notice that those points located close to the axis, have a higher

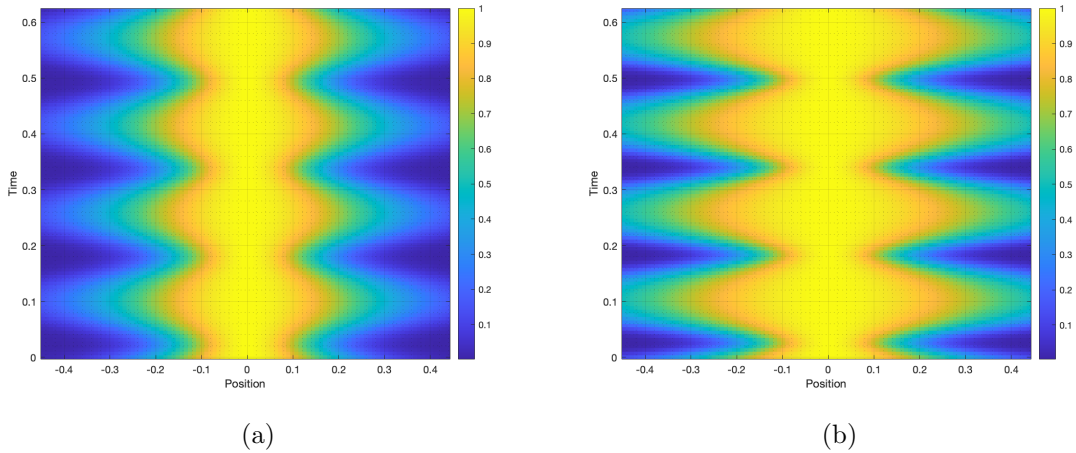


Figure 1: Heat map of the function  $|\Psi_\xi(x, t)|^2$ . In (1a)  $r = 0.5$  and  $r = 1$  in (1b), illustrating the effect of the squeezing parameter  $r$ , both cases with  $\phi = 60^\circ$ .

probability and the effect of the squeezing parameter in shrinking some regions whereas it expands others. There is abundant literature on the properties and main features of this state [19, 20, 21]. Let us now move towards the next section and obtain Bohm's equation and its solution.

### 3 Bohmian analysis

In this section we are going to introduce the analysis of the particles' trajectories using the Bohmian equations [1, 2, 3] and then we are going to analyze a scenario in which a position detection is performed. Let us recall that in Bohm's description, the quantum particles have well defined trajectories and velocities. For a single particle in 1D, the Bohm equation is given as

$$m \frac{dq}{dt} = -\hbar \operatorname{Im} \left( \frac{\partial_x \Psi(x, t)}{\Psi(x, t)} \right) \Big|_{x=q}, \quad (29)$$

where  $\Psi(x, t)$  is the wave function or the pilot wave in the Bohmian mechanics context. In our case, replacing the pilot wave by the time evolved squeezed state in Eqn (26) gives the following equation

$$\dot{q}(t) = \frac{\omega \tanh(2r) \sin(2\omega t - \phi)}{1 - \tanh(2r) \cos(2\omega t - \phi)} q(t), \quad (30)$$

whose solution is of the form

$$q(t) = q_0 \sqrt{\frac{1 - \tanh(2r) \cos(2\omega t - \phi)}{1 - \tanh(2r) \cos \phi}}, \quad (31)$$

here  $q_0$  is the initial condition and notice that the period of the trajectories doubles the period of the classical harmonic oscillator system used in the time evolution of the state in Eqn (24). In Figure (2) we plotted some of the trajectories using this solution and with initial conditions distributed according to the initial state in Eqn (17). The figure shows the resemblance with the plot of the wave function given in Figure (1).

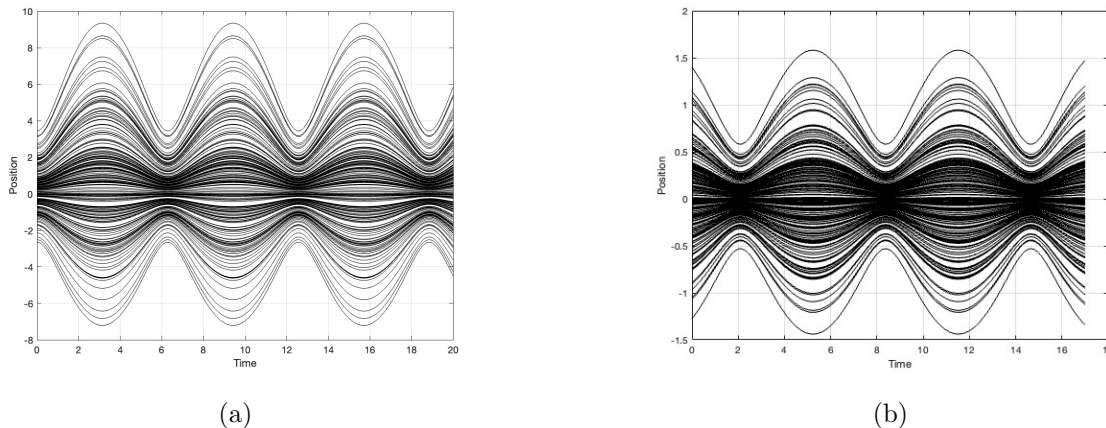


Figure 2: Bohmian trajectories of the squeezed state in Eqn (26) using the square of the wave function in Eqn (17) for the probability distribution of the initial conditions. In (a) the phase  $\phi = 0$  and in (b) the phase  $\phi = 2\pi/3$ . In both cases we plotted  $n = 200$  trajectories with  $\hbar = m = 1$  and  $\omega = 0.5$  and a squeezed parameter value of  $r = 0.5$ .

Using the state in Eqn (17) for the distribution of the initial conditions is what is called the Bohm thermal equilibrium postulate in which it is stated that not only the wave function is used to derive the Bohm's equations as in Eqn (29) but also that the initial conditions must obey a probability distribution which is not uniform but given by the initial state.

Apart from the fact that the trajectories do not cross or touch each other, there are some features of this solution worth to be mentioned. Regarding the initial conditions, (i) If  $q_0 = 0$ , then  $q(t) = 0$  for any  $t \geq 0$  but the converse is not true: having  $q(t) = 0$  for some  $t$  does not imply that  $q_0 = 0$ . (ii) If  $q_0 > 0$  (or  $q_0 < 0$ ) then  $q(t) > 0$  (or  $q(t) < 0$ ) for any  $t \geq 0$ , that is, if we have positive initial conditions then the positions will be positive positions, and viceversa, if we have positive positions they were generated only by positive initial conditions. Similarly for the negative positions counterpart. (iii) The initial conditions squeeze the trajectories upwards or downwards and the period is constant in all the cases:  $T = \pi/\omega$ .

Regarding the values of the squeezing parameter  $r$ , (i) for a given squeezing parameter  $r > 0$ , the trajectories are squeezed, mostly at those time intervals in which the function  $q(t)$  reaches its minimum and expanded on the maximum values. (ii) When  $r \rightarrow 0$ , we obtain that

$$\lim_{r \rightarrow 0} q(t) = q_0, \quad (32)$$

which indicates that the particle *is not moving* and that its position remains at the initial position where the particle was emitted. The reason for this is that this limit corresponds to the vacuum state in Eqn (16) where the particle has a well defined energy  $E_0 = \frac{\hbar\omega}{2}$ . This implies that the time evolved wave function is a product of two functions, a time dependent phase  $e^{-\frac{iE_0 t}{\hbar}}$  and the position dependent initial quantum state  $\Psi_0(x)$ . Hence the gradient term in Eqn (29) leaves the time dependent function unaltered thus cancelling the imaginary contributions. As a result, once we carry out an experiment and measure a given value of the position, we are just detecting the initial position in which the particle was emitted. This is a standard result when considering energy eigenstates in the Bohmian formalism. (iii) In the case where  $r \rightarrow \infty$ , we obtain that

$$\lim_{r \rightarrow \infty} q(t) = q_0 \left| \frac{\sin(\omega t - \phi/2)}{\sin(\phi/2)} \right|, \quad (33)$$

which becomes singular at  $\phi = 0$  and  $t \neq n\pi + \phi/2$ .

As mentioned before, the thermal equilibrium hypothesis in Bohm's formalism indicates that the initial positions are distributed according to the initial state given, in this case, by the Eqn (17). Therefore, once a particle is detected, we cannot predict its initial condition and due to the initial conditions cannot be predicted, we cannot use the trajectories to predict where the particle will be anytime. In this regard, both descriptions of quantum mechanics, the Bohmian and the standard interpretations coincide.

Consider that a particle is emitted at some unknown initial position  $q_0$  and the parameters  $r$ ,  $\phi$ ,  $l$  are fixed. According to the Eqn (31), the maximum and the minimum positions the particle can reach for a given albeit unknown initial condition are

$$q_{max} = q_0 \sqrt{\frac{1 + \tanh(2r)}{1 - \tanh(2r) \cos(\phi)}}, \quad q_{min} = q_0 \sqrt{\frac{1 - \tanh(2r)}{1 - \tanh(2r) \cos(\phi)}}, \quad (34)$$

therefore, due to  $q_0$  cannot be predicted the maximum and the minimum values cannot be predicted either. Of course, the initial condition  $q_0$  must be such that  $q_{min} \leq q_0 \leq q_{max}$ . This condition is always fulfilled due to

$$\sqrt{1 - \tanh(2r)} \leq \sqrt{1 - \tanh(2r) \cos(\phi)} \leq \sqrt{1 + \tanh(2r)}, \quad (35)$$

for any  $r \geq 0$  and  $\phi \in [0, 2\pi)$ .

In Figure (3a) we plotted the trajectories in the phase space  $(q(t), \dot{q}(t))$  for different values of the initial conditions. We can notice in Figure (3b) the effect of having larger values of initial

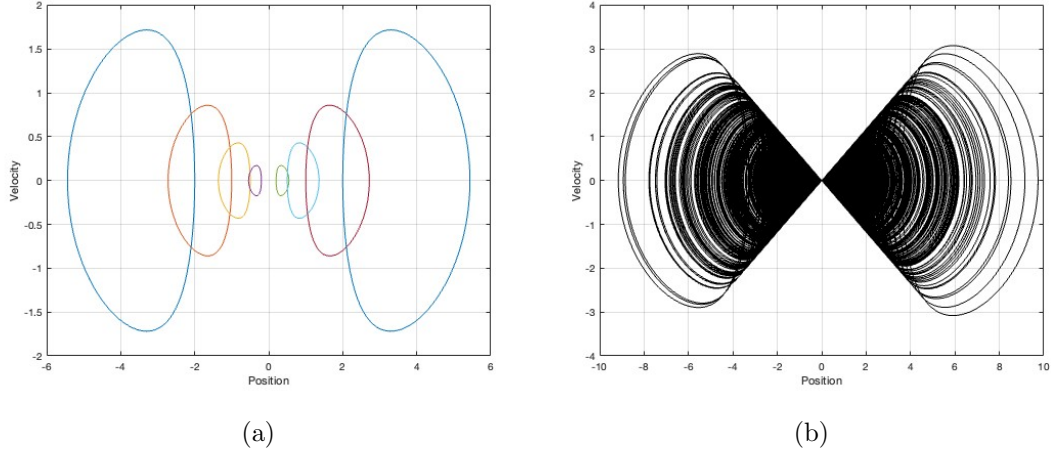


Figure 3: Bohmian trajectories of the squeezed state in Eqn (26) using the square of the wave function in Eqn (17) for the probability distribution of the initial conditions. In (a) the phase  $\phi = 0$  and in (b) the phase  $\phi = 2\pi/3$ . In the second case we plotted  $n = 200$  trajectories and in both we have:  $\hbar = m = 1$ ,  $\omega = 0.5$  and a squeezed parameter value of  $r = 0.5$ . The purpose of (a) is to show the shape of individual trajectories whereas in (b) its collective shape of the trajectories.

conditions upon the trajectories: the largest the initial condition, the largest the maximum and the lowest minimum velocities of the system as well. Actually, we found a forbidden region in the phase space delimited by the lines

$$\dot{q}_{\pm} = \pm 2\omega \sinh(2r) q. \quad (36)$$

We are intrigued about the role of this region when considering the multiple Fourier modes of the quantum free field (for example a real free scalar field). In particular, its role when considering the Lorentz symmetry. However, such analysis is beyond the scope of our present work.

Up to this point, notice the similarity between the classical and the quantum Bohmian description in the sense that both give rise to closed trajectories in the phase space and therefore, the positions (as well as the velocities) are bounded. The standard approach to quantum mechanics cannot foresee this feature as it predicts a continuum unbounded spectrum for the position operator. This *bounded-ness* of the Bohmian trajectories influences the time of arrival of the particles, in particular due to the fact that the period in both cases depends only on the inverse frequency. Even more, if there is a time arrival detection, this time will have an upper bound. Let us explore all these aspects in the next subsection.

### 3.1 Detection at a given position $L$

Consider the scenario in which the Bohmian particle was detected at some position  $L > 0$  (this happens of course at finite time). We do not know what the initial condition was, but we do know that the initial condition associated with the trajectory followed by the particle is in a subset given by those initial conditions such that  $L = q(t_{oa}, q_0)$  for some finite time  $t_{oa}$ . Later on we will relate this time  $t_{oa}$  with the time of arrival of the Bohmian particle.

From Eqn (31) it can be checked that the minimum value of the initial condition, denoted by  $q_0^{min}$ , such that the maximum position of its trajectory is  $L$  is given by

$$q_0^{min}(r, \phi, L) = L \sqrt{\frac{1 - \tanh(2r) \cos(\phi)}{1 + \tanh(2r)}}, \quad (37)$$

and similarly, the maximum value of the initial condition, denoted by  $q_0^{max}$ , such that the minimum position of its trajectory is  $L$  is given by

$$q_0^{max}(r, \phi, L) = L \sqrt{\frac{1 - \tanh(2r) \cos(\phi)}{1 - \tanh(2r)}}. \quad (38)$$

Hence, if the particle was detected at position  $L$ , despite not knowing the initial condition, the Bohmian formalism predicts that the initial condition belongs to the interval

$$q_0 \in [q_0^{min}(r, \phi, L), q_0^{max}(r, \phi, L)], \quad (39)$$

see Figure (4) for some illustration examples. Notice that due to both  $q_0^{min}$  and  $q_0^{max}$  linearly depend on  $L$ , the interval length is also a linear function of  $L$ , hence when  $L$  increases the length of the interval linearly increases and therefore, *more* initial conditions *can participate* in the detection events.

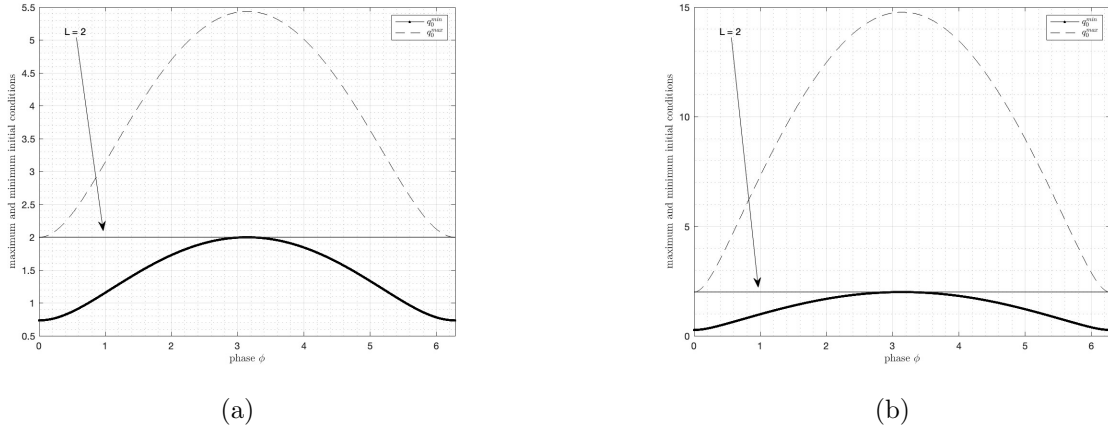


Figure 4: Maximum initial condition (dashed line) and minimum initial conditions (solid line) as functions of the phase  $\phi$ , see Eqn (37) and Eqn (38). In (a) the squeezing parameter  $r = 0.5$  and in (b)  $r = 1$  and in both cases  $L = 2$ . This plot shows that all the trajectories detected at  $L = 2$  will have initial conditions lying between these two curves for any  $\phi$ .

Additionally, there is a value of the phase, denoted as  $\phi_c(r)$ , in which the length of the interval formed with the initial conditions above  $L$  equals the length of the interval formed with those initial conditions below  $L$ . This phase value is found as a solution of the relation

$$\cos(\phi_c(r)) = \frac{(2 \cosh^2(r) + 1) (\cosh(r) - 1)}{\sinh(2r) \cosh^2(r)}. \quad (40)$$

This shows that the initial conditions values are distributed differently around the detection position  $L$ . When  $\phi < \phi_c(r)$ , then  $q_0^{max} - L < L - q_0^{min}$  and when  $\phi > \phi_c(r)$ , then  $q_0^{max} - L > L - q_0^{min}$ . On the other hand, from Eqn (37) and Eqn (38), we notice that

$$\lim_{r \rightarrow 0} q_0^{min}(0, \phi, L) = \lim_{r \rightarrow 0} q_0^{max}(0, \phi, L) = L, \quad (41)$$

indicating that in this limit the particle will be detected at  $L$  if and only if it was emitted exactly at  $q_0 = L$ . However, we will see further below that this limit is a singular one. Moreover, when  $r \rightarrow \infty$  we have that

$$\lim_{r \rightarrow \infty} q_0^{min}(r, \phi, L) = L |\sin(\phi/2)|, \quad \lim_{r \rightarrow \infty} q_0^{max}(r, \phi, L) = \begin{cases} L & \text{if } \phi = 0 \\ \infty & \text{if } \phi \neq 0 \end{cases}, \quad (42)$$

which shows that taking the phase value  $\phi = 0$  and then the limit  $r \rightarrow \infty$  yields a result different to the one obtained when taking the limit first and then evaluate  $\phi = 0$ . Finally, when  $\phi = 0$  the interval in Eqn (39) is finite while it ranges from a finite value at  $L|\sin(\phi/2)|$  to infinity when  $\phi \neq 0$ .

## 4 Time of arrival

We now state the following question: what time would it take for the particle to reach this position  $L$  for the first time? Let us call this *time of arrival*<sup>2</sup> and let us denote it as  $t_{oa}$ . We can obtain this time by inverting the function in Eqn (31) and considering the principal branch of the arccos function

$$t_{oa}(q_0) = \frac{1}{2\omega} \left\{ \phi + \arccos \left[ \frac{1}{\tanh(2r)} \left\{ 1 - [1 - \tanh(2r) \cos(\phi)] \frac{L^2}{q_0^2} \right\} \right] \right\}, \quad (43)$$

and this holds as long as  $q_0 \in [q_0^{min}, q_0^{max}]$ , which is the domain of  $t_{oa}(q_0)$  and because otherwise, the time taken to reach  $L$  will be infinite, i.e., it is undefined.

Let us now explore  $t_{oa}$  as a function of the initial condition  $q_0$ . If we evaluate  $t_{oa}$  at the initial positions given in Eqn (37) and Eqn (38) in Eqn (43) we obtain

$$t_{oa}(q_0^{min}) = \frac{\phi + \pi}{2\omega}, \quad t_{oa}(q_0^{max}) = \frac{\phi}{2\omega}, \quad (44)$$

which indicates that when the  $\phi < \pi$  then the maximum time for a particle to reach  $L$  is  $t_{oa}(q_0^{min})$  and when the phase  $\phi > \pi$  then the maximum time for a particle to reach  $L$  is  $t_{oa}(q_0^{max})$ . Consequently, no matter how long  $L > 0$  is, as long as there is a detection, the maximum time taken for a particle to reach this position is upper bounded. In both cases, the minimum time is always  $t_{oa} = 0$ .

An important aspect of these time values is that they do not depend on the parameter  $r$ . As a consequence, the limits  $r \rightarrow 0$  and  $r \rightarrow \infty$  do not alter these values. However, if we consider the limit  $r \rightarrow 0$ , then from Eqn (41) we know that the initial conditions tend to  $L$  indicating that there is only one possible time of arrival given by  $t_{oa} = 0$ , as there will be only one particle emitted at  $L$ . But on the other hand, from Eqn (44) we notice that this is not the case. As a result, we have to consider the limit  $r \rightarrow 0$  as a singular one for the function in Eqn (43). Of course, this singular behavior results from the inverse function used to solve the parameter  $t$  from the Eqn (31) and the factor of  $\tanh(2r)$  in the denominator so nothing of real physical relevance is happening here. The lesson is that when considering the function in Eqn (43), we have to take the limit  $r \rightarrow 0$  as a singular point<sup>3</sup>.

An observation worth to consider is that due to the domain of the function in Eqn (44) is the interval in Eqn (39), no time value can be derived for initial conditions out of this interval. What can we formally do to consider those initial conditions  $q_0 \notin [q_0^{min}, q_0^{max}]$ ? What we consider a natural option to answer this is to construct the time function as a piecewise function of the form

$$t_{fa}(q_0) = \begin{cases} \frac{\phi + \arccos \left[ \frac{1}{\tanh(2r)} \left\{ 1 - [1 - \tanh(2r) \cos(\phi)] \frac{L^2}{q_0^2} \right\} \right]}{2\omega} & \text{if } q_0 \in [q_0^{min}, q_0^{max}], \\ \infty & \text{if } q_0 \notin [q_0^{min}, q_0^{max}], \end{cases} \quad (45)$$

<sup>2</sup>We do not explore *how* this time measurement is performed. We are just assuming it can be done and if so, what will be the consequences in light of the Bohmian interpretation.

<sup>3</sup>The singularity emerges due to in the limit  $r \rightarrow 0$  the inverse function arccos becomes multivalued.

hence indicating that the particle will never reach the position  $L$  if  $q_0 \notin [q_0^{min}, q_0^{max}]$ . However, as we will see further below, this brings a scenario in which the probability for these time values becomes problematic and some additional constraints are needed. Recall that, we cannot consider as null the time values for the initial positions out of the interval  $[q_0^{min}, q_0^{max}]$  due to this implies that the particles indeed reached the position  $L$  because they were emitted exactly at  $L$  in a similar way to what we have explained when  $r = 0$ . The physical situation here is rather different and that is why we have to consider this approach.

Let us now continue with the analysis and recall that up to this point, we have only considered one detection event, so let us consider that we repeat this process many times. Each experiment performed with the same values of  $L$ ,  $r$  and  $\phi$  and each time we collect the values of the time of arrival  $t_{oa}$  of the particles. Our questions are now the following: (i) what would be the probability distribution of these time of arrivals? and (ii) what is the mean value of the times collected? Let us address these questions in the following subsection.

#### 4.1 Time of arrival statistics

The probability distribution of the time of arrival has been defined in many references (see for example [14, 15, 16, 17, 18]) when adapted to the Bohmian description. Denoted as  $\Pi_\xi(t)$  in the present case, its expression is given by

$$\Pi_\xi(\tau) = \frac{\int_{\text{supp}\Psi_\xi} \delta(t(q_0) - \tau) |\Psi_\xi(q_0)|^2 dq_0}{Z}, \quad (46)$$

where  $t_{min}$  and  $t_{max}$  are the extremes of the interval  $[\frac{\phi+\pi}{2\omega}, \frac{\phi}{2\omega}]$  according to the values in the Eqn (44) and the normalization factor  $Z$  is given by

$$Z = \int_{t_{min}}^{t_{max}} \left[ \int_{\text{supp}\Psi_\xi} \delta(t(q_0) - \tau) |\Psi_\xi(q_0)|^2 dq_0 \right] dt. \quad (47)$$

Once we substitute the expression for  $\Psi_\xi(q_0)$  and  $t(q_0) = \tau$  in Eqn (46) we obtain the following expression for  $\Pi_\xi(\tau)$

$$\Pi_\xi(\tau) = \frac{L\omega \sinh(2r) \sin(2\omega\tau - \phi) e^{-\frac{L^2}{l^2[\cosh(2r) - \sinh(2r) \cos(2\omega\tau - \phi)]}}}{Z\sqrt{\pi} l [\cosh(2r) - \sinh(2r) \cos(2\omega\tau - \phi)]^{3/2}} \quad (48)$$

and in Figure (5) we show its graph as a function of  $\omega\tau - \phi$ .

From Figure (5a) we can extract out the following observations, (i)  $\Pi_\xi(\tau)$  has a global maximum value at, say  $\tau_{max}$ , (ii) increasing  $r$  moves  $\tau_{max}$  to the left indicating that the most probable time of arrival decreases with increasing  $r$ . This result can be observed in Figure (6a) where we showed the values of the mean time of arrival as a function of the squeezing parameter  $r$  and for different values of the ratio  $L/l$ . (iii) the value of  $\Pi_\xi(\tau_{max})$  increases with increasing  $r$ . Figure (5b) on the other hand shows a very different behavior. First, the distribution will always present a global maximum  $\Pi_\xi(\tau_{max})$  for every value of  $L$ , however, when  $L$  increases the value  $\tau_{max}$  moves now to the right. Additionally, when increasing  $L$  the values of  $\Pi_\xi(\tau_{max})$  first decrease and then, after a certain value of  $L$  it reaches the infimum value among the values of  $\Pi_\xi(\tau_{max})$  and then it starts increasing again.

In Figure (6b) we plotted the values of the mean time of arrival but as a function of the ratio  $L/l$  and for different values of  $r$ . The subfigure (6a) shows that

$$\lim_{r \rightarrow \infty} \langle t_{oa} \rangle = \frac{\phi}{2\pi}, \quad (49)$$

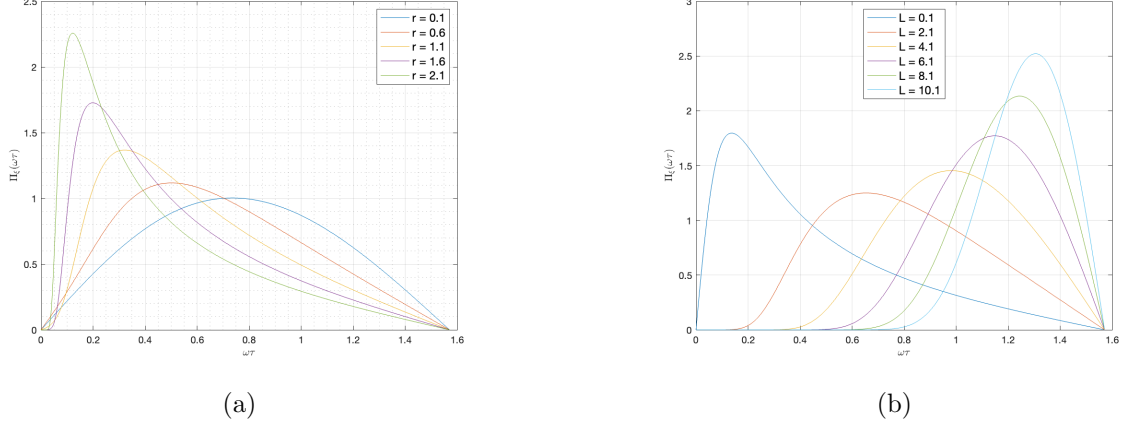


Figure 5: Probability distribution of Time of Arrival  $\Pi_\xi$  as a function of  $\omega\tau$ . In (5a) we varied the squeezing parameter  $r$  and consider  $L = 1$  fixed. In (5b) we fixed  $r = 1$  and  $L$  changes. In both cases,  $\hbar = m = 1$ ,  $\omega = 0.5$  and  $\phi = 0$ .

and this value constitutes a lower bound for  $\langle t_{oa} \rangle$ . Figure (6b) on the other hand, shows an upper bound for a every fixed value of  $r$ , when the limit  $L/l \rightarrow \infty$  is taken

$$\lim_{L/l \rightarrow \infty} \langle t_{oa} \rangle = \frac{\phi + \pi}{2\pi}. \quad (50)$$

For small values of  $r$ , Figure (6a) shows that

$$\lim_{r \rightarrow 0} \langle t_{oa} \rangle = \frac{\pi + \phi}{2\omega}, \quad (51)$$

for any  $L/l$  value but as we know, in this limit, the inverse *arccos* function is not well defined hence it constitutes a singular limit. All these limits have in common that they do not depend on the parameters  $r$  or  $L$ . however, the limit of small  $L/l$ , as can be seen in Figure (6b) shows that it will depend on the  $r$  value fixed.

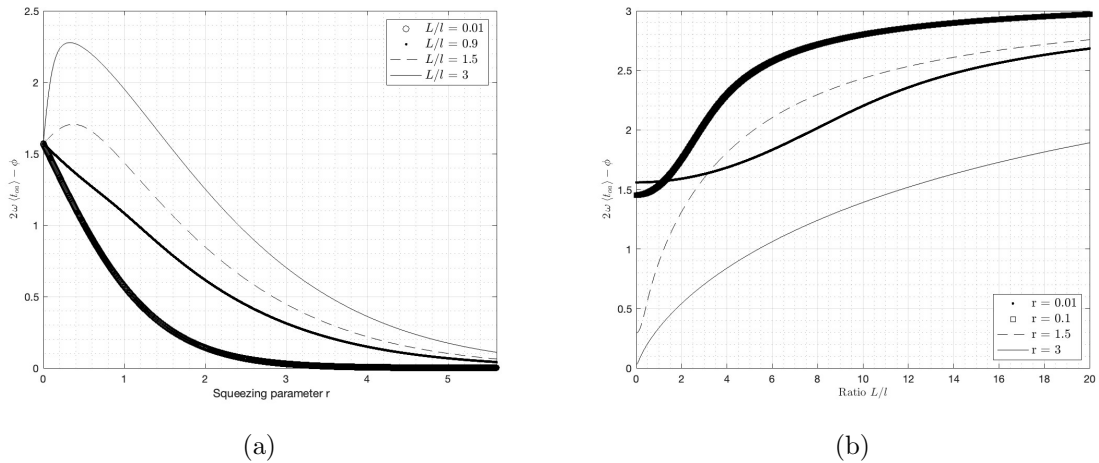


Figure 6: In (5a) we plotted  $2\omega\langle t_{oa} \rangle - \phi$  as a function of the squeezing parameter  $r$  for different values of the ratio  $L/l$ . In (5b) we plotted  $2\omega\langle t_{oa} \rangle - \phi$  as a function of the ratio  $L/l$  but for different values of the squeezing parameter  $r$ .

Let us now observe the following: Eqn (48) imposes some constraints on the distribution of the initial conditions giving rise to trajectories able to click the detector at  $L$ . To better understand these results, let us consider the mean value of the time of arrival which is given by

$$\langle t_{fa} \rangle = \int \tau \Pi_{\xi}(\tau) d\tau, \quad (52)$$

and let us re-write this expression in terms of the  $q_0$  coordinates using the relation  $t(q_0) = \tau$ , which reads as

$$\langle t_{fa} \rangle = \frac{\int_{q_0^{min}(L)}^{q_0^{max}(L)} \left\{ \frac{\phi + \arccos \left[ \frac{1}{\tanh(2r)} \left\{ 1 - [1 - \tanh(2r) \cos(\phi)] \frac{L^2}{q_0^2} \right\} \right]}{2\omega} \right\} |\Psi_{\xi}(q_0)|^2 dq_0}{\int_{q_0^{min}(L)}^{q_0^{max}(L)} |\Psi_{\xi}(q_0)|^2 dq_0}, \quad (53)$$

where  $\Psi_{\xi}(q_0)$  is the state given in Eqn (17) but replacing  $x$  by  $q_0$  and restricting its domain to the integration interval. This expression can be interpreted as the mean value of the function  $t(q_0)$  with probability distribution given by

$$Pr(Q = q_0) = \begin{cases} \frac{|\Psi_{\xi}(q_0)|^2 dq_0}{\int_{q_0^{min}(L)}^{q_0^{max}(L)} |\Psi_{\xi}(q_0)|^2 dq_0} & \text{if } q_0 \in [q_0^{min}(L), q_0^{max}(L)] \\ 0 & \text{if } q_0 \notin [q_0^{min}(L), q_0^{max}(L)] \end{cases} \quad (54)$$

This result affects our interpretation of the probability for the initial conditions as follows: the initial conditions participating in the detection event at  $L$  are not distributed according to Eqn (17) but according to the distribution given in Eqn (54). The reason for this is because those  $q_0 \notin [q_0^{min}, q_0^{max}]$  must have a null probability to happen because otherwise, their time of arrival will yield an undefined value. Therefore, only those  $q_0 \in [q_0^{min}, q_0^{max}]$  have to be considered as physical detection events. As a consequence, the initial condition should be updated which requires the normalization factor in Eqn (54).

In Bayesian terms, Bohmian mechanics offer more information about the system, which in this case consists in the realization of a position interval for the initial conditions out of which the time taken for the particle to reach the position  $L$  is infinite. This *new information* about the system drives us to update our information of the probabilities for the different time values to happen as seen in the Eqns (46) and (53). If, on the other hand, we decide to integrate over the entire real line in Eqn (53) without changing the values of the probabilities, then a mathematical inconsistency emerges due to imaginary time values associated with the initial positions out of the domain of the time function. This is an immediate conclusion according to our Bohmian results: we are forced to update the probability distribution for the initial conditions or otherwise the mathematical prediction is inconsistent.

## 5 Discussion and conclusions

Let us dig in a bit more into the consequences of the prediction of such an interval in the Bohmian formalism. First, recall that in the standard quantum approach, the position operator spectra is unbounded and no such interval can emerge. When a detector is placed at the position  $L$ , and the particles are produced at  $t = 0$  according to the state in Eqn (17) and then time-evolved according to the state in Eqn (26), there is no way to discriminate amid the initial position values because there are no trajectories to begin with and the particles are delocalized over the entire real line. Consequently, if we change the position of the detector, the

number of particles reaching the detector changes but according to the probability distribution in Eqn (26) (now evaluated at the new position) and not due to any constraint on the particles' trajectory. For example, let us consider the following *Gedanken experiment*:

- Let us produce a particle at  $t = 0s$  (all the parameters fixed  $\lambda = \{r, \phi, \omega, \dots\}$ ) described with the state in Eqn (17). The detector, placed at  $L$ , is turned on also at  $t = 0$  (i.e., particle production and turning on the detector are synchronised events).
- As time goes by, the quantum state evolves according to Eqn (26) and the particle will hit the detector. We do not know where the particle will hit, neither when, but we can turn the detector off after a time  $T = \pi/\omega$ , after of which any detection will be registered. We then repeat this experiment, say  $N$  times after of which we collect the number of clicks  $N_c(L, T; \lambda)$  in the detection screen for the same window of time  $t \in [0, T]$ .
- According to the standard interpretation of quantum mechanics, the number of detection events in the interval  $(L, L + dL)$  at time  $t$  is given by

$$|\Psi_\xi(x = L, t)|^2 dL, \quad (55)$$

and  $x \in \mathbb{R}$ . Hence, if we consider the entire time interval  $[0, T]$  we have

$$N_c(L, T; \lambda) = \frac{dL}{T} \int_0^T |\Psi_\xi(L, t)|^2 dt \quad (56)$$

Notice that the number of clicks do not depend on any notion to an interval constraining the value of the positions. This of course is not the case in the Bohmian approach presented here.

- In the Bohmian interpretation, the number of clicks for the interval  $(L, L + dL)$  is actually proportional to the *number* of possible initial conditions which can actually hit the detector,

$$\frac{|\Psi_\xi(x = L, t)|^2 dL}{\int_{q_0^{min}(L)}^{q_0^{max}(L+dL)} dq_0 |\Psi_\xi(q(t; q_0), t)|^2}, \quad (57)$$

where  $q(t; q_0)$  is the Bohmian trajectory given in Eqn (31). If we consider the entire time interval we have

$$N_c^{(B)}(L, T; \lambda) = \frac{dL}{T} \int_0^T dt \frac{|\Psi_\xi(x = L, t)|^2}{\int_{q_0^{min}(L)}^{q_0^{max}(L+dL)} dq_0 |\Psi_\xi(q(t; q_0), t)|^2} \quad (58)$$

As can be seen, the relations in Eqn (56) and Eqn (58) are rather different from which we can expect different predictions.

The second consequence of this result is related with the role of the detection event and the equilibrium hypothesis. If no detector is placed, then the initial conditions are distributed according to the state in Eqn (17). Once a detector is introduced and placed at  $L$ , according to the Bohm's solution for the system, not all the initial conditions will reach the detector, only those in an interval linearly dependent in  $L$ . These initial conditions will yield trajectories with a well defined time of arrival of particles at the detector. The distribution of these initial conditions differs from the one given in Eqn (17) and can only be obtained via the Bohmian solution. This fact indicates that in order to obtain this probability distribution one has to

accept that the information provided by the wave function as in Eqn (17) or in Eqn (26) is not complete.

There are, of course, other conclusions worth to mention in particular regarding the time of arrival distribution and the mean time of arrival. The first one is that the probability distribution  $\Pi_{\xi}(\tau)$  has a maximum and a minimum arrival time resulting from the boundeness of the trajectories as explained before. We can expand the domain of this function given in Eqn (48), for example for  $\tau \in [0, +\infty)$  but it results in altering the multiple counting events. Therefore, if the detector is placed at  $L$ , then the first time of arrival (if it clicks the detector) will be smaller than  $t_{max}$  and this time value is related with the times of arrival given in Eqn (44) depending on the squeezing phase  $\phi$ . Notably, the squeezing phase can alter the value  $t_{max}$  which is an unexpected role for this parameter.

We consider our results to be the first step towards a deeper analysis linking the squeezed states and the time of arrival measurements. Going further towards higher degrees of freedom systems and also towards considering a model for the detector is the natural next step. Moreover, we hope that the ubiquitous use of squeezed states in quantum optics experiments might open the doors for an experimental realization confirming or denying any of our predictions.

## Acknowledgments

AGCH would like to thank the CONAHCyT for a postdoctoral fellowship.

## References

- [1] James T Cushing, Arthur Fine, and Sheldon Goldstein. *Bohmian mechanics and quantum theory: an appraisal*, volume 184. Springer Science & Business Media, 1996.
- [2] Detlev Dürr, Sheldon Goldstein, Roderich Tumulka, and Nino Zanghí. Bohmian mechanics. In *Compendium of quantum physics*, pages 47–55. Springer, 2009.
- [3] Albert Benseny, Guillermo Albareda, Ángel S Sanz, Jordi Mompart, and Xavier Oriols. Applied bohmian mechanics. *The European Physical Journal D*, 68:1–42, 2014.
- [4] Yakir Aharonov and David Bohm. Time in the quantum theory and the uncertainty relation for time and energy. *Physical Review*, 122(5):1649, 1961.
- [5] Jerzy Kijowski. On the time operator in quantum mechanics and the heisenberg uncertainty relation for energy and time. *Reports on Mathematical Physics*, 6(3):361–386, 1974.
- [6] J Gonzalo Muga, S Brouard, and D Macias. Time of arrival in quantum mechanics. *Annals of Physics*, 240(2):351–366, 1995.
- [7] V Delgado and JG Muga. Arrival time in quantum mechanics. *Physical Review A*, 56(5):3425, 1997.
- [8] V Delgado. Probability distribution of arrival times in quantum mechanics. *Physical Review A*, 57(2):762, 1998.
- [9] Yakir Aharonov, Jonathan Oppenheim, Sandu Popescu, Benni Reznik, and WG Unruh. Measurement of time of arrival in quantum mechanics. *Physical Review A*, 57(6):4130, 1998.

- [10] V Delgado. Quantum probability distribution of arrival times and probability current density. *Physical Review A*, 59(2):1010, 1999.
- [11] Juan Gonzalo Muga and C Richard Leavens. Arrival time in quantum mechanics. *Physics Reports*, 338(4):353–438, 2000.
- [12] Mathieu Beau, Maximilien Barbier, Rafael Martellini, and Lionel Martellini. Time-of-arrival distributions for continuous quantum systems and application to quantum back-flow. *Physical Review A*, 110(5):052217, 2024.
- [13] Norbert Grot, Carlo Rovelli, and Ranjeet S Tate. Time of arrival in quantum mechanics. *Physical Review A*, 54(6):4676, 1996.
- [14] WR McKinnon and CR Leavens. Distributions of delay times and transmission times in bohm’s causal interpretation of quantum mechanics. *Physical Review A*, 51(4):2748, 1995.
- [15] Siddhant Das and Detlef Dürr. Arrival time distributions of spin-1/2 particles. *Scientific reports*, 9(1):2242, 2019.
- [16] Siddhant Das, Markus Nöth, and Detlef Dürr. Exotic bohmian arrival times of spin-1/2 particles: An analytical treatment. *Physical Review A*, 99(5):052124, 2019.
- [17] Aurélien Drezet. Arrival time and bohmian mechanics: It is the theory which decides what we can measure. *Symmetry*, 16(10):1325, 2024.
- [18] M Ruggenthaler, G Grübl, and S Kreidl. Times of arrival: Bohm beats kijowski. *Journal of Physics A: Mathematical and General*, 38(39):8445, 2005.
- [19] Daniel F Walls. Squeezed states of light. *nature*, 306(5939):141–146, 1983.
- [20] Roman Schnabel. Squeezed states of light and their applications in laser interferometers. *Physics Reports*, 684:1–51, 2017.
- [21] Christopher C Gerry and Peter L Knight. *Introductory quantum optics*. Cambridge university press, 2023.
- [22] Marcos Moshinsky and Christiane Quesne. Linear canonical transformations and their unitary representations. *Journal of Mathematical Physics*, 12(8):1772–1780, 1971.
- [23] Kurt Bernardo Wolf. Development of linear canonical transforms: a historical sketch. In *Linear Canonical Transforms*, pages 3–28. Springer, 2016.
- [24] Amalia Torre. *Linear ray and wave optics in phase space: bridging ray and wave optics via the Wigner phase-space picture*. Elsevier, 2005.
- [25] Guillermo Chacón-Acosta and Angel Garcia-Chung. The relation between the symplectic group  $sp(4, r)$  and its lie algebra: Applications to polymer quantum mechanics. *Physical Review D*, 104(12):126006, 2021.